Protic Ionic Liquids and Salts as Versatile Carbon Precursors

Shiguo Zhang, Muhammed Shah Miran, Ai Ikoma, Kaoru Dokko, and Masayoshi Watanabe*

Department of Chemistry and Biotechnology, Yokohama National University, Hodogaya-ku, Yokohama 240-8501, Japan

S *Supporting Information*

ABSTRACT: Instead of traditional polymer precursors and complex procedures, easily prepared and widely obtainable nitrogen-containing protic ionic liquids and salts were explored as novel, small-molecule precursors to prepare carbon materials (CMs) via direct carbonization without other treatments. Depending on the precursor structure, the resultant CMs can be readily obtained with a relative yield of up to 95.3%, a high specific surface area of up to 1380 m^2/g, or a high N content of up to 11.1 wt%, as well as a high degree of graphitization and high conductivity (even higher than that of graphite). One of the carbons, which possesses a high surface area and a high content of pyridinic N, exhibits excellent electrocatalytic activity toward the oxygen reduction reaction in an alkaline medium, as revealed by an onset potential, half-wave potential, and kinetic current density comparable to those of commercial 20 wt% Pt/C. These low-cost and versatile precursors are expected to be important building blocks for CMs.

Carbon materials (CMs), which are prepared by the carbonization of C-containing precursors, have been extensively used in diverse areas such as environmental treatment, catalysis, gas capture/storage, and energy conversion/storage.[1] To satisfy such applications, great effort has been focused on the discovery of precursors and appropriate methods to obtain CMs with a controlled structure, regulated texture, graphitic framework, large specific surface area and pore volume, and desirable heteroatom doping.[2] Particularly, the precursors play a crucial role, and their chemical composition is often reflected in the type and amount of heteroatoms found in the final CMs. For example, one can easily incorporate dopants, such as nitrogen,[3] into the CM structure by choosing appropriate precursor molecules. Despite works related to the synthesis, the study of organic precursors has been less emphasized in the past,[2b,4] mainly because most organic compounds are evaporated or decomposed into gaseous products before/during high-temperature carbonization. The current precursors available are therefore rather limited to only a few sources: (a) The most popular precursors are low-vapor-pressure natural or synthetic polymers such as polyacrylonitrile,[5] and phenolic resins,[6] which pose certain difficulties because of their limited solubility and complicated synthesis. (b) Alternatively, synthetic polymers can be synthesized in situ from polymerizable monomers such as furfuryl alcohol,[2] and acrylonitrile.[7] However, a specific compound, a prepolymerization step prior to carbonization, and additional acid or metal catalysts are necessary. The slow procedures and metal impurities are unfavorable for actual

applications. The graphitization and N content are also somewhat insufficient because of the inherent nature of the limited CM precursors.[2b,4] (c) Small molecules with high volatility such as acetonitrile and benzene can also be used as precursors to prepare CMs, particularly nanostructured CMs such as carbon nanotubes, while harsh conditions such as chemical vapor deposition (CVD) are crucial.[8] (d) Recently, ionic liquids (ILs) were shown to be excellent precursors due to their negligible volatility, high thermal stability, and molecular tunability,[9] which facilitate the carbonization process, resulting in CMs with a high N content, conductivity,[9,10] and potential for applications in catalysis and electrochemistry.[11] Unfortunately, only very few cyano/nitrile-containing aprotic ILs could yield CMs.[9a,12] The multistep and time-consuming synthesis, rigorous purification, metal impurities (e.g., Li, Na, or Ag, possibly from metathesis), and high cost may complicate their manufacture and hinder large-scale production.

Herein, we report that protic ILs and salts (PILs/PSs) can be used as novel, low-molecular weight organic precursors for the direct synthesis of CMs (Figure 1a). In contrast to conventional precursors, PILs/PSs possess negligible volatility, comparable to that of aprotic ILs, but are easily obtained and widely available. The structural diversity of PILs/PSs also enables us to investigate the correlation between the precursor structures and the properties of the final CMs, which allows the synthesis of specific CMs with controlled structure and properties.
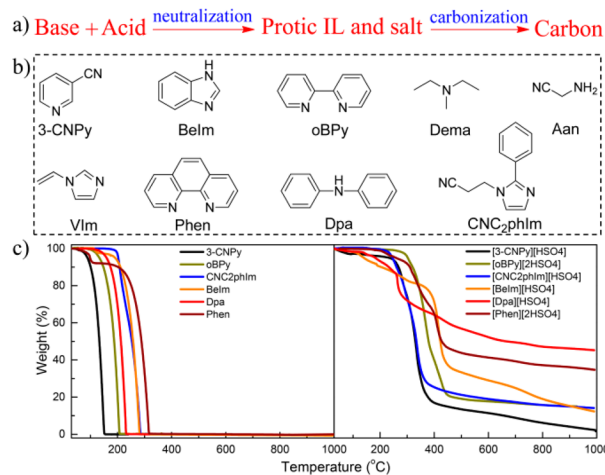

Figure 1. (a) Representation of the PILs/PSs-based strategy. (b) Structures of the N-containing bases being investigated. (c) Thermal gravimetric analysis curves of typical PILs/PSs.

All PILs/PSs were synthesized by stoichiometric neutralization of the respective N-containing bases with H_2SO_4 and subsequent removal of the solvent. The resulting products were subjected to direct carbonization at 1000 °C. Thermal gravimetric analysis of the PILs/PSs is shown in Figure 1c. Clearly, all the parent bases were completely evaporated or decomposed below 400 °C, as expected. In contrast, the corresponding PILs/PSs yielded CM residues, with absolute (oven) and relative (oven/theoretical) yields up to 46.0% ([Dpa][HSO_4]) and 95.3% ([Phen][2HSO_4], Table S1, Supporting Information [SI]), respectively. The CM yield appears to vary significantly with the nature of the base. Bases containing the thermally stable benzene moieties gave much higher yields than aliphatic amines and heterocycles, even those containing cross-linkable moieties (C≡N, C=C). This is not unexpected, considering that, in polymer precursors, the benzene-containing polymers/blocks are always original CM sources upon carbonization, while the aliphatic polymers/blocks act as sacrificial components and/or templates to generate porosity via alkyl chain cleavage. From the results of the diverse PILs/PSs listed in Table S1, we can conclude that most N-containing bases could be protonated to behave as potential CM precursors, even those with a very low molecular weight and a low boiling point, for which low yields but high surface areas were obtained (e.g., [Dema][HSO_4] and [Aan][HSO_4], Table S1). The only exception we found are PILs/PSs with a very high N content (usually N/C > 1), which were unable to produce CMs. Alternatively, they were first transformed into polymeric carbon nitrides around 550 °C and then decomposed above 800 °C (Figure S3: [taPyim][H_2SO_4], N/C = 1.5).[13]

N-doped CMs are currently attracting much attention because conjugation between the N lone-pair and the π-system of the C lattice can dramatically alter or improve the physicochemical properties of the CMs such as the conductivity, basicity, oxidative stability, and catalytic activity.[3,14,15] In situ preparation from N-containing precursors offers the advantage of easier control of the incorporated N, which is usually more homogeneously distributed throughout the material compared to those obtained by the post-treatment method that requires additional complex and time-consuming steps.[14] The unique compositions of the PILs/PSs herein happen to allow the fabrication of intrinsic N-doped CMs. As confirmed by elemental analysis, all the PILs/PSs can yield N-containing CMs, and the N content varies significantly, depending on the precursors, between ~2.1 and 11.1 wt% at 1000 °C (Table S1). In particular, the CM derived from [3-CNPy][HSO_4] exhibits a very high N content of 11.1 wt %. To our knowledge, such a high content has never been achieved in a one-step synthesis of N-doped CMs from a single organic source, although 12.0 wt% could be obtained by co-carbonization of natural N-rich compounds.[11a] Considering that [3-CNPy][HSO_4] has a N/C molar ratio as low as 0.33, about half that of [EMIm][DCA] (0.63),[9b] the high N content in the resulting CM is surprising and indicates that at least 30% of the N atoms originally present in the precursor were finally incorporated within the CM architecture. Although no exact correlation of the N content between the PILs/PSs and the final CMs was found, the high N content in the CMs derived from both [3-CNPy][HSO_4] and [oBPy][2HSO_4] (9.5 wt% of N in CM and incorporation of 50% of the N atoms of the precursor) suggests that not only the nitrile group, as reported,[9] but also the pyridine moiety behave as sources of N and may improve the final N fixation. The lower N content in the CMs from aliphatic amine-based precursors further confirmed this point, due to the
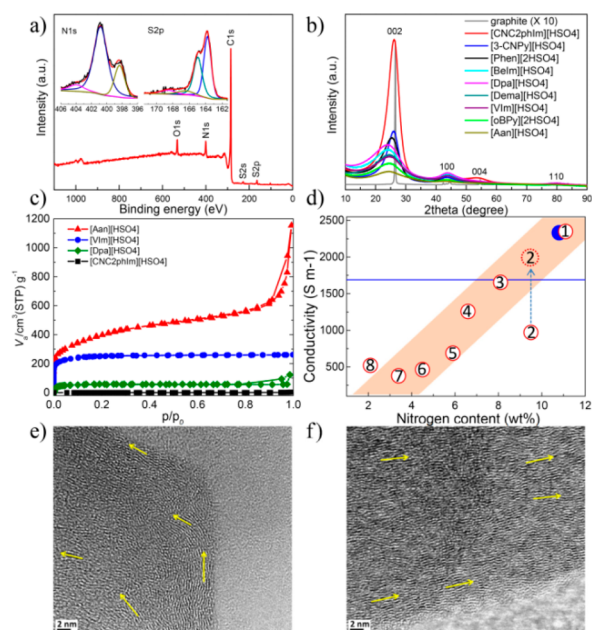
Figure 2. (a) XPS spectra of [3-CNPy][HSO_4]-based carbon materials. (b) XRD patterns, (c) N_2 sorption isotherms, and (d) relative conductivity of the CMs derived from PILs/PSs. **1**, [3-CNPy][HSO_4]; **2**, [oBPy][2HSO_4]; **3**, [CNC_2phIm][HSO_4]; **4**, [Phen][2HSO_4]; **5**, [BeIm][HSO_4]; **6**, [Dpa][HSO_4]; **7**, [VIm][HSO_4]; **8**, [Dema]-[HSO_4]. Red dashed circle = estimated conductivity of CM **2** from the general relationship between N content and conductivity. (Blue circle) [EMIm][DCA]-based CM and (blue line) graphite. High-resolution transmission electron microscopy images of CMs derived from (e) [3-CNPy][HSO_4] and (f) [CNC_2phIm][HSO_4].

facile decomposition of pendant alkylamino groups (e.g., via Hofmann elimination) that are covalently bound to the CM with a weak C−N bonding energy.

Further investigation by X-ray photoelectron spectroscopy (XPS) indicated that N atoms are structurally integrated into the CM matrix. As shown in Figure 2a, the N environments in the CM derived from [3-CNPy][HSO_4] are dominated by pyridinic N (398.3 eV) and quaternary N (400.8 eV). The slight impurity at higher energy (404.0 eV) is probably oxidized N species.[4b] Besides the N, C, and O detected by XPS, all the CMs also contain a small amount of sulfur (Table S2), ranging from 0.4 to 2.3 at.%. The S2p peak can be resolved into four compositions at binding energies of 163.8, 165.0, 166.4, and 168.6 eV (inset in Figure 2a). The former two peaks correspond to the S2p$_{3/2}$ and S2p$_{1/2}$ of thiophene, while the weak peaks at higher binding energy are minor contributions from oxidized sulfur species.[16] This simple method indeed provides a facile route to synthesize N and S bifunctional CM for potential applications.[17] The obtained CMs vary from nonporous to porous, depending on the precursor structures (Figure 2c). Although all CMs are microporous (Figure 2c), some of them exhibit high specific surface area (S_{BET}). For example, the [Aan][HSO_4]-based CM possesses a S_{BET} as high as 1380 m^2/g. As shown in Figure 2c, its N_2 sorption shows a typical Type I isotherm with two sharp uptakes at low ($p/p_0 < 0.15$) and high ($p/p_0 < 0.9$) relative pressure, respectively, indicating that it is a microporous material with some small macropores. Taking into account that highly porous CMs can only be achieved via a nanocasting method or activation, this facile one-step method is of great significance.

X-ray diffraction (XRD) was performed on all the CMs (Figure 2b). Judging from the Bragg reflection of the (002) peak,

the CMs with higher N content, e.g., [3-CNPy][HSO$_4$], [Phen][2HSO$_4$], and [CNC$_2$phIm][HSO$_4$]-based CMs, display a more positive shift of the diffraction position, higher intensity, and narrower line width and thus are more graphitic (Table S2). In particular, the [CNC$_2$phIm][HSO$_4$]-based CM shows a high-intensity (002) diffraction peak centered at 26.2°, along with clearly observable (100), (004), and (110) reflections characteristic for graphitic structures. The calculated interlayer distance (d_{002}) of 0.339 nm is very close to that of graphite.[18] Such a high degree of graphitization has never been reported by one-step carbonization.[19] A crude estimate of the lateral size (L_a) of the nanographitic domains based on the width of the (100) peak by the Scherrer equation indicated that they did not exceed 1.6 nm. Likewise, the mean stack height (L_c) estimated by the (002) peak was ~1.8 nm, indicating that single crystallites were composed of approximately five π-stacked nanographene sheets.[20] High-resolution transmission electron microscopy provided further evidence that these CMs are made up of bent graphite-like sheets, which are uniformly present throughout the entire CM structure (Figure 2e,f). The most remarkable feature is the somewhat "one direction" arrangement of the graphene layers in the [CNC$_2$phIm][HSO$_4$]-based CM due to its high degree of graphitization, while in the [3-CNPy][HSO$_4$]-based CM, they are much more randomly oriented (arrows in Figure 2). It is important to note that graphite-like microstructures were obtained under mild conditions without additional graphitization treatments such as complex graphite-like precursors,[2b,4b] catalytic graphitization,[21] CVD,[22] or very high temperature.[23] The high crystallinity obtained here for the highly N-doped CMs is unexpected since it is generally accepted that the incorporation of a large number of N atoms in a C lattice results in the amorphization of the graphitic network, which may lead to a bent CM structure with a relatively long interlayer distance.[17,25] Indeed, CMs with a high N content ([3-CNPy][HSO$_4$], [oBPy][2HSO$_4$], [CNC$_2$phIm][HSO$_4$], and [Phen][2HSO$_4$]) appear to show much wider Raman G and D bands than those with a lower N content, suggesting that N-doping imparts a new structural irregularity to the hexagonal rings and, consequently, many defects in the graphene layers (Figure S6 and Table S4), as expected. However, XPS spectra revealed that the CMs from [3-CNPy][HSO$_4$], [CNC$_2$phIm][HSO$_4$], and [Phen][2HSO$_4$] have a relatively higher pyridinic N content but a lower quaternary N content than others (Figure S6). It is known that pyridinic N is planar while quaternary N has an "out-of-plane" bonding configuration.[24] Thus, the above three CMs with a high pyridinic N content, owing to their planar structure, possess short interlayer distances. In contrast, the [oBPy][2HSO$_4$]-based CM, with a high N content, shows a weak, broad (002) signal, which is common in most PILs/PSs-based CMs (Figure 2b) and often related to an amorphous nature, as confirmed by electron diffraction measurements (Figure S7).[19] This can be explained by its relatively high content of three-dimensional quaternary N, which results in curvature and local distortion of the graphene layer and thus a loss of packing density (Figure S6).

Considering both the high degree of graphitization and the high N content, these CMs are expected to be highly conductive. The electrical conductivities of all the CMs were measured under the same conditions (see SI). As shown in Figure 2d, the conductivity is interestingly found to be roughly proportional to the N content in CMs (orange region in Figure 2d), due to the doping effect of electron-rich N that induced a donor state above the Fermi energy level and increased its electron density.[15,25,26] For example, CMs **1**−**4**, having high N content, generally exhibit

higher conductivity than CMs **5**−**8**. Graphitization can further improves the conductivity, as revealed by [CNC$_2$phIm][HSO$_4$]-based CM, which has the highest degree of graphitization and thus a conductivity comparable to graphite. In particular, the [3-CNPy][HSO$_4$]-based CM, possessing the highest N content and relatively high degree of graphitization, is even much more conductive than graphite. This result is very similar to that seen with [EMIm][DCA]-based CM (Figure 2d).[9b] In contrast, [oBPy][2HSO$_4$]-based CM (**2**), in spite of its high N content (9.5 wt%), exhibits a much lower conductivity than expected (Figure 2d), which is certainly ascribed to its low degree of graphitization as revealed by XRD.

Because carbonization is a complicated process wherein multiple chemical reactions occur simultaneously,[27] the detailed carbonization process of PILs/PSs may differ substantially depending on their respective structure, producing distinct CMs in terms of yield, N content, porosity, and graphitic structure, as stated above. In an attempt to clarify the carbonization mechanism, [CNC$_2$phIm][HSO$_4$], which contains various distinct but common moieties, was selected as a typical precursor, and its products obtained at various temperatures were carefully investigated (see SI). It was found that during carbonization, the thermally unstable moieties such as alkyl chains, cyano functional groups, anions and heterocyclic imidazolium rings were first decomposed at a low temperature, and the in situ-formed fragments further underwent a number of transformations (e.g., cross-linking polymerization and recombination) and partially condensed and/or fused with the thermally stable domains, e.g., benzene, to form N-containing polycyclic aromatic compounds and finally transform into N-doped CMs via denitrogenation, desulfuration, and dehydrogenation. It should be noted that the high proton transfer energy from the strong sulfuric acid to the nitrogenous base is also essential to improve the thermal stability of the PILs/PSs under the harsh carbonization to achieve high CM yield.[28] In combination with the detailed discussion about the CM nature, it was speculated that PILs/PSs with heterocycles, cyano groups, and benzene groups (or fused aromatic structures) are liable to yield CMs with a high N content and a high degree of graphitization (and thus a high conductivity). In contrast, those with aliphatic moieties usually led to highly porous CMs, wherein the pore was formed at the expense of the anions and the thermally unstable moieties in the cations. The incorporation of structural N may additionally improve the expected functional N species.

The as-prepared N-doped porous CM from [Aan][HSO$_4$] (A-NPC) exhibited excellent electrocatalytic activity toward the oxygen reduction reaction (ORR), as evaluated by cyclic voltammetry (CV) and rotating ring-disk electrode (RRDE) measurements. As shown in Figure 3, a quasi-rectangular voltammogram without any significant redox peak within the potential range from −1.0 to +0.2 V was observed in the N$_2$-saturated 0.1 M KOH solution, as a result of the typical supercapacitance of highly porous CMs.[2c,11a,17] In contrast, a well-defined cathodic peak at −0.220 V vs Ag/AgCl (−0.162 V for commercial 20 wt% Pt/C) emerges in the CV as the electrolyte is saturated with O$_2$. Further experiments by RRDE revealed that the ring current for A-NPC from peroxide oxidation was very small (Figure 3). The calculated peroxide yield from the RRDE data was <15%, and the average electron transfer number (n) is >3.7 for A-NPC over the range from −1.0 to −0.2 V (Figure S15), confirming that the ORR proceeds through a mainly four-electron reduction pathway. Moreover, A-NPC exhibits an onset potential and a half-wave potential at −0.078
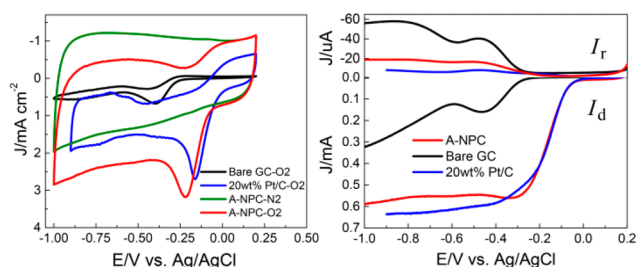
Figure 3. CV (100 mV/s) and RRDE results (1600 rpm and 10 mV/s) of bare, glassy C, A-NPC, and commercial 20 wt% Pt/C in O_2-saturated 0.1 M KOH solution. The catalyst loading is 127 $\mu g/cm^2$ for A-NPC and 25.4 $\mu g_{Pt}/cm^2$ for Pt/C.

and −0.157 V, respectively, very close to that of Pt/C (Figure 3). The Tafel slope in the low current density region of A-NPC is 78 mV per decade, close to the value of 75 mV per decade for the Pt/C catalyst (Figure S15). The kinetic current densities at −0.09 V (vs Ag/AgCl) for A-NPC and Pt/C, calculated after correcting for the diffusion-limiting current, were 0.77 and 0.75 mA/cm^2 (Figure S15). Furthermore, metal-free A-NPC shows long-term durability superior to Pt/C (Figure S15). The ORR performance for A-NPC is obviously much better than most of the reported C-based catalysts that require special templates and complicated synthetic steps,[2c,17] thus strongly demonstrating its pronounced electrocatalytic activity. This is probably because of its high S_{BET} and high content of pyridinic N, which facilitated mass transport and provided a high surface density of catalytic sites for the ORR (Figure S6). The high sulfur content on the A-NPC surface (Table S2) may give rise to additional contributions due to the possible synergistic activation of C atoms by S and N dual-doping.[17]

In conclusion, the PILs/PSs demonstrated herein are simple, low cost, and versatile precursors for the generation of carbon materials without any complicated synthesis, catalyst, template, or other complex techniques. The correlation between the precursors and the nature of the CMs was preliminarily investigated in terms of yield, porosity, N content, graphitic structure, and conductivity in order to possibly tailor the CMs at the molecular level. This strategy is very easily scaled up for mass production and could pave the way for developing novel CMs through suitable combinations of acids and bases. One of the N-doped nanoporous CMs, A-NPC, found immediate potential application as a highly efficient metal-free catalyst for the oxygen reduction reaction in an alkaline medium.

■ ASSOCIATED CONTENT

Ⓢ Supporting Information
Experimental details and characterization data. This material is available free of charge via the Internet at http://pubs.acs.org.

■ AUTHOR INFORMATION

Corresponding Author
mwatanab@ynu.ac.jp

Notes
The authors declare no competing financial interest.

■ ACKNOWLEDGMENTS

■ REFERENCES

(1) (a) Ryoo, R.; Joo, S. H.; Kruk, M.; Jaroniec, M. *Adv. Mater.* **2001**, *13*, 677. (b) Liang, C. D.; Li, Z. J.; Dai, S. *Angew. Chem., Int. Ed.* **2008**, *47*, 3696.

(2) (a) Joo, S. H.; Choi, S. J.; Oh, I.; Kwak, J.; Liu, Z.; Terasaki, O.; Ryoo, R. *Nature* **2001**, *412*, 169. (b) Kim, C. H.; Lee, D. K.; Pinnavaia, T. J. *Langmuir* **2004**, *20*, 5157. (c) Liu, R. L.; Wu, D. Q.; Feng, X. L.; Mullen, K. *Angew. Chem., Int. Ed.* **2010**, *49*, 2565.

(3) Gong, K. P.; Du, F.; Xia, Z. H.; Durstock, M.; Dai, L. M. *Science* **2009**, *323*, 760.

(4) (a) Zhai, Y. P.; Wan, Y.; Cheng, Y.; Shi, Y. F.; Zhang, F. Q.; Tu, B.; Zhao, D. Y. *J. Porous Mater.* **2008**, *15*, 601. (b) Kim, T. W.; Park, I. S.; Ryoo, R. *Angew. Chem., Int. Ed.* **2003**, *42*, 4375.

(5) Kowalewski, T.; Tsarevsky, N. V.; Matyjaszewski, K. *J. Am. Chem. Soc.* **2002**, *124*, 10632.

(6) Liang, C. D.; Hong, K. L.; Guiochon, G. A.; Mays, J. W.; Dai, S. *Angew. Chem., Int. Ed.* **2004**, *43*, 5785.

(7) Lu, A. H.; Kiefer, A.; Schmidt, W.; Schuth, F. *Chem. Mater.* **2004**, *16*, 100.

(8) Zhang, W. H.; Liang, C. H.; Sun, H. J.; Shen, Z. Q.; Guan, Y. J.; Ying, P. L.; Li, C. *Adv. Mater.* **2002**, *14*, 1776.

(9) (a) Lee, J. S.; Wang, X. Q.; Luo, H. M.; Baker, G. A.; Dai, S. *J. Am. Chem. Soc.* **2009**, *131*, 4596. (b) Paraknowitsch, J. P.; Zhang, J.; Su, D. S.; Thomas, A.; Antonietti, M. *Adv. Mater.* **2010**, *22*, 87.

(10) (a) Lee, J. S.; Wang, X. Q.; Luo, H. M.; Dai, S. *Adv. Mater.* **2010**, *22*, 1004. (b) Wang, X. Q.; Dai, S. *Angew. Chem., Int. Ed.* **2010**, *49*, 6664. (c) Fechler, N.; Fellinger, T. P.; Antonietti, M. *Adv. Mater.* **2013**, *25*, 75.

(11) (a) Yang, W.; Fellinger, T. P.; Antonietti, M. *J. Am. Chem. Soc.* **2011**, *133*, 206. (b) Fellinger, T. P.; Hasche, F.; Strasser, P.; Antonietti, M. *J. Am. Chem. Soc.* **2012**, *134*, 4072. (c) Xu, X.; Li, Y.; Gong, Y.; Zhang, P.; Li, H.; Wang, Y. *J. Am. Chem. Soc.* **2012**, *134*, 16987.

(12) Wooster, T. J.; Johanson, K. M.; Fraser, K. J.; MacFarlane, D. R.; Scott, J. L. *Green Chem.* **2006**, *8*, 691.

(13) Thomas, A.; Fischer, A.; Goettmann, F.; Antonietti, M.; Muller, J. O.; Schlogl, R.; Carlsson, J. M. *J. Mater. Chem.* **2008**, *18*, 4893.

(14) Shao, Y. Y.; Sui, J. H.; Yin, G. P.; Gao, Y. Z. *Appl. Catal., B* **2008**, *79*, 89.

(15) Yang, Q. H.; Xu, W. H.; Tomita, A.; Kyotani, T. *Chem. Mater.* **2005**, *17*, 2940.

(16) Paraknowitsch, J. P.; Wienert, B.; Zhang, Y. J.; Thomas, A. *Chem.—Eur. J.* **2012**, *18*, 15416.

(17) Liang, J.; Jiao, Y.; Jaroniec, M.; Qiao, S. Z. *Angew. Chem., Int. Ed.* **2012**, *51*, 11496.

(18) Gogotsi, Y.; Nikitin, A.; Ye, H. H.; Zhou, W.; Fischer, J. E.; Yi, B.; Foley, H. C.; Barsoum, M. W. *Nat. Mater.* **2003**, *2*, 591.

(19) Yoon, S. B.; Chai, G. S.; Kang, S. K.; Yu, J. S.; Gierszal, K. P.; Jaroniec, M. *J. Am. Chem. Soc.* **2005**, *127*, 4188.

(20) Knox, J. H.; Kaur, B.; Millward, G. R. *J. Chromatogr.* **1986**, *352*, 3.

(21) Iyer, V. S.; Vollhardt, K. P. C.; Wilhelm, R. *Angew. Chem., Int. Ed.* **2003**, *42*, 4379.

(22) Xia, Y. D.; Mokaya, R. *Adv. Mater.* **2004**, *16*, 1553.

(23) Kyotani, M.; Matsushita, S.; Nagai, T.; Matsui, Y.; Shimomura, M.; Kaito, A.; Akagi, K. *J. Am. Chem. Soc.* **2008**, *130*, 10880.

(24) Ding, W.; Wei, Z.; Chen, S.; Qi, X.; Yang, T.; Hu, J.; Wang, D.; Wan, L.-J.; Alvi, S. F.; Li, L. *Angew. Chem., Int. Ed.* **2013**, *52*, 11755.

(25) Czerw, R.; Terrones, M.; Charlier, J. C.; Blase, X.; Foley, B.; Kamalakaran, R.; Grobert, N.; Terrones, H.; Tekleab, D.; Ajayan, P. M.; Blau, W.; Ruhle, M.; Carroll, D. L. *Nano Lett.* **2001**, *1*, 457.

(26) Wiggins-Camacho, J. D.; Stevenson, K. J. *J. Phys. Chem. C* **2009**, *113*, 19082.

(27) Moldoveanu, S. C. *Pyrolysis of Organic Molecules with Applications to Health and Environmental Issues*; Elsevier: Amsterdam, Netherlands, 2010.

(28) Miran, M. S.; Kinoshita, H.; Yasuda, T.; Susan, M. A.; Watanabe, M. *Phys. Chem. Chem. Phys.* **2012**, *14*, 5178.